Atmospheric circulation modulates the spatial variability of temperature in the Atlantic-Arctic region

Impact of weather regimes on temperature in the Atlantic-Arctic region

Olivier Champagne[1, 2, *], Benjamin Pohl[2], Shawn McKenzie[1], Jean-François Buoncristiani[2], Eric Bernard[3], Daniel Joly[3], Florian Tolle[3]

1. School of Geography and Earth Sciences, McMaster University, Hamilton, Ontario, Canada
2. Biogéosciences, CNRS, université de Bourgogne Franche-Comté, Dijon, France
3. ThéMA, CNRS, université de Bourgogne Franche-Comté, Besançon, France

***Corresponding Author:** Olivier Champagne
Burke Science Building, Room 313, McMaster University
1280 Main Street West, Hamilton, Ontario, L8S 4K1, Canada
Email: champago@mcmaster.ca; Tel: (905) 525-9140, ext. 27879

Abstract

The Arctic region has experienced significant warming during the past two decades with major implications on the cryosphere. The causes of Arctic amplification are still an open question within the scientific community, attracting recent interest. The goal of this study is to quantify the contribution of atmospheric circulation on temperature variability in the Atlantic Arctic region at decadal to intra-annual timescales from 1951 to 2014. Daily 20th Century reanalyses geopotential height anomalies at 500hPa were clustered into different weather regimes to assess their contribution to observed temperature variability. The results show that, in winter, 25% of the warming (cooling) in the North Atlantic Ocean (northeastern Canada) is due to temporal decreases of high geopotential anomalies in Greenland. This regime influences air mass migration patterns, bringing less cold (warm) air masses into these regions. Additionally, atmospheric warming or cooling has been attributed to a change in nearby oceanic basin surface conditions because of sea ice decline. In summer, about 15% of the warming observed in Norwegian/Greenland Seas is related to an increase in temporal anticyclonic patterns. This ratio reaches 37% in Norway due to an amplification from downward solar radiation. This study allows for better understanding how natural climate

This article has been accepted for publication and undergone full peer review but has not been through the copyediting, typesetting, pagination and proofreading process which may lead to differences between this version and the Version of Record. Please cite this article as doi: 10.1002/joc.6044

variability modulates the regional signature of climate change and estimating the uncertainties in climate projections.

Keywords: Weather Regimes, Atmospheric Circulation, Atlantic-Arctic, Reanalyses, Internal Climate Variability, Arctic Amplification

1. Introduction

Glacier and ice cap mass loss in response to climate change majorly contributes to sea level rise (Mernild et al., 2010), which is likely to continue (Meier et al., 2007). In the Arctic, observed atmospheric warming is particularly pronounced (Holland & Bitz, 2003; Bekryaev et al., 2010; Pithan & Mauritsen, 2014) leading to significant reduction of snow, glacial and sea ice volume in high latitudes (Kaser et al., 2006; Screen & Simmonds, 2010). These changes are particularly significant in Greenland (Rignot et al., 2011; Bezeau et al., 2015; Sasgen et al., 2012), the Canadian Arctic Archipelago (Gardner et al., 2011; Bezeau et al., 2015) and Spitsbergen (Kohler et al., 2007; James et al., 2012). The origin of observed Arctic warming is inconclusive, but has been attributed to shifts in oceanic circulation (Mahajan et al., 2011), temperature and albedo feedback (Pithan & Mauritsen, 2014), and increased heat flux from the oceans due to sea ice loss (Screen & Simmonds, 2010; Lang et al., 2017; Ogawa et al., 2018; Sun et al., 2018). Atmospheric circulation has also been discussed as a past warming tracer in many Arctic regions (Bezeau et al., 2015; Ding et al., 2017; Fettweis et al., 2011; Hanna et al., 2013, 2018; Isaksen et al., 2016; McLeod et al., 2018; Overland et al., 2012; Overland & Wang, 2016). Large-scale atmospheric variability modes, such as the North Atlantic oscillation (NAO), partly drove the twentieth century temperature variability in Arctic subploar regions (Hurrell & Deser, 2010). However, since the 1990's, the link between NAO and temperature is less clear (Ding et al., 2017). Other atmospheric variability

indices have been introduced recently to explain the Arctic amplification in summer. The Arctic Dipole (AD), characterized by low pressure anomalies in the Siberian Arctic and high pressure anomalies over the Beaufort Sea, caused meridional winds and a warming in Greenland and northeastern Canada (Overland et al., 2012). The Greenland Blocking index (GBI), defined as a quasi-stationary anticyclone that persists a few days in Greenland, was also associated with the warming (Hanna et al., 2018). In Alaska, summer warming was partly associated to the meridional advection of heat and moisture due to the recurrence of the Alaskan Blocking Index (ABI) (McLeod et al., 2018). The recent warming amplification observed in the Arctic in summer have been clearly associated with high pressure anomalies (Bezeau et al., 2015; Ding et al., 2017; Fettweis et al., 2011; Hanna et al., 2013; Overland et al., 2012). During winter, temperature extremes observed in past years have been partly attributed to atmospheric circulation (Isaksen et al., 2016; Overland & Wang, 2016; Ogawa et al., 2018; Sun et al., 2018). Generally, atmospheric patterns accompanied with increased water vapor may enhance downward infrared radiations (IR), increasing temperature in winter (Yao et al., 2018). Following this mechanism, the strong warming over the Barents Sea was partly attributed to the temporal persistence of a Blocking over the Ural region (D. Luo et al., 2016), primarily in conjunction with a positive phase of the North Atlantic Oscillation (NAO) (B. Luo et al., 2017).

Previous studies using large scale indices such as Arctic Dipole, Blocking or NAO, can only discuss a low range of large-scale flow variability (Papritz & Grams, 2018). Other atmospheric circulation classifications, used recently in the Arctic, cover a larger range of large-scale atmospheric variability (Papritz & Grams, 2018). These methods include Self

organizing maps (Bezeau et al., 2015; Mioduszewski et al., 2016), circulation type classifications (Fettweis et al., 2011; Isaksen et al., 2016), or weather regimes classifications (Crasemann et al., 2017; Guemas et al., 2010; Papritz & Grams, 2018). These classifications allow to deconstruct the long-term evolution of climate into a limited number of robust patterns of recurrent meteorological systems. Weather regimes, specifically, identify the most robust and recurrent properties (location, intensity, persistence) of the meteorological systems (high and low pressure) (Michelangeli et al., 1995), and allows to study the frequency at which the weather patterns occur over diverse temporal scales (Pohl & Fauchereau, 2012). Weather regimes have been extensively used in middle latitudes (Yiou & Nogaj, 2004; Cassou et al., 2005; Grams et al., 2017; Raymond et al., 2018; Vigaud et al., 2018; Alvarez-Castro et al., 2018). Guemas et al., (2010) successfully implemented this technique in the North Atlantic region, showing temporal recurrence of specific weather regimes and how their properties influence sea surface temperature. Weather regimes classification was also used to investigate the cold outbreak formation in the northeast portion of North-Atlantic basin (Papritz & Grams, 2018) and to analyze sea ice volume impact on atmospheric patterns occurrences (Crasemann et al., 2017). These studies do not consider the pre-1979 period (Crasemann et al., 2017; Papritz & Grams, 2018), or the very recent years (Guemas et al., 2010) and are limited to one season. Our objective is to complement these studies by determining robust weather regimes over the Atlantic Arctic region (-80°W to +90°E longitude, +50°N to +90°N latitude) and how they relate to atmospheric temperature changes from 1951 to 2014 at seasonal to decadal timescale. Specifically, we examine whether recent

Arctic amplification can be explained by changes in weather regime frequency or other intrinsic properties (i.e. temperature anomalies).

This paper is organized as follows: Section 2 presents the data applied in this work and the k-means algorithm used to construct robust weather regimes. Section 3 examines the characteristics of weather regime patterns and explores their temporal frequency (inter-annual and decadal). Section 4 examines how the spatial variability of temperature in the Arctic is related to properties of weather regimes. Section 5 includes our concluding remarks.

2. Data and Method

2.1. Weather regime computation

The weather regimes constructed for this study are shown as maps of the most recurrent and robust variability patterns of the Atlantic Arctic region atmosphere (-80°W to +90°E longitude, +50°N to +90°N latitude) (Figure 1). These regimes are constructed from daily geopotential height anomalies at 500 hPa (Z500 hereafter) and document the most robust geographic location and intensity of anticyclones (positive geopotential height anomalies against the climatological mean) and depressions (negative anomalies). These atmospheric fields are derived from the 20th Century Reanalysis version 2 (20CR hereafter) at a resolution of 2° x 2° from December 1950 to November 2014. The record prior to 1950 is not used because of larger uncertainties due to the lower amount of observational data assimilated and constraining the atmospheric fields (Compo et al., 2011). Selected variables also include 2m surface air temperature, 10m surface wind, downward infrared radiation (IR), downward shortwave radiation (SR), cloud water content, and total cloud cover. Cloud water content is

used instead of total column water vapor, because 20CR daily total column water is not available. These data are used to calculate anomalies synchronous to the occurrence of each regime. All anomalies are tested using a two-sided Student's *t* test.

To evaluate the 20CR regimes, the weather regimes are computed using the ERA-Interim reanalysis (ERAI, Dee et al., 2011) from 1979 to 2014. ERAI has a higher resolution (0.75° × 0.75°), assimilated larger amounts of observed or remote-sensed data, and shows lower uncertainties and errors. Our study focuses on the Atlantic side of the Arctic, allowing for future analyses on weather regimes impact on the Spitsbergen cryosphere. In previous studies, a distinctive domain for the Pacific and the Atlantic side of the Arctic were useful when examining mid-latitude circulation on subarctic weather variability (Oudar et al., 2017). The first attempts at using large-scale North Atlantic regimes, with domains extending from the tropics (23°N) to the North Pole (Cassou et al., 2004), provided less satisfactory results because the region of interest (the Atlantic Arctic) was too peripheral.

The regimes are determined by the so called "k-means" algorithm (Michelangeli et al., 1995). This algorithm constructs statistically robust maps representing recurrent atmospheric configurations. Maps are constructed by minimizing the intra-class heterogeneity using an iterative process. The number of regimes to be retained is determined by a "red-noise test" conducted through the comparison of observed atmospheric anomalies maps with numerically-generated atmosphere, that have the same statistical properties (e.g. serial correlation) (Michelangeli et al., 1995). According to this test, six regimes are identified as the most significant for the full year. Similar tests determine six regimes for the warm season (April to September) and seven regimes for the cold season (October to March). The six

regimes obtained in summer are similar to six of the seven regimes calculated for the winter season, and also to the seven regimes obtained by Grams et al., (2017) for the whole year. For conciseness and because the seasonal definition of the regime does not improve the analysis, only the six regimes calculated for the whole year are used hereafter. In particular, the contribution of the regime frequency to long-term changes in the Arctic climate is not qualitatively modified between seasonal and yearly definitions of the regimes (not shown).

2.2. Temperature dataset experiment

Theoretical daily temperatures are constructed for each of the 21 × 91 grid-points of the domain based on the influence of weather regimes and referred to hereafter as the experiment dataset (EXP). For each grid-point, the mean temperature corresponding to each regime for the period of 1951-2014 is first computed monthly using 20CR daily 2-meters atmospheric temperatures. These mean-monthly temperatures are then assigned to each day of the 64-year study period according to the month and the regime that occurs. This method was recently used to quantify how observed trends of temperature or precipitation can be explained by changes in atmospheric circulation (Fleig et al., 2015). The method was successfully applied to Europe (Nilsen et al., 2017; Murawski et al., 2018) and central Asia (Gerlitz et al., 2018). Daily surface temperatures from 20CR are used to estimate the observed change of temperature from 1951 to 2014 for each grid-point during each season (names CTL for control). The significance of the inter-annual temperature trend for the EXP and CTL as well as regime occurrences are tested seasonally by the Spearman's rank correlation test (hereafter referred to as Spearman test).

The ratio of EXP to CTL linear temperature trends is calculated for each grid-point for the entire 64-year period (1951-2014). To assess the robustness of end-point yearly intervals, calculations are replicated by excluding either the first or last single, two, or three years from the 64 years period, giving a total of ten different possibilities. The linear temperature ratio is considered robust for a grid point when the standard deviation is lower than 25% of the ten averaged combinations. This method reveals the grid locations where the calculated trend is highly dependent on the first and last years of the time series. Analyses that rely on temperature trends in these areas should be taken with caution.

3. Results

3.1. The Atlantic-Arctic weather regimes

Six weather regimes were identified as significant and consist of the most robust meteorological systems in the domain. Figure 1 presents the Z500 anomalies associated with the six regimes derived from 20CR reanalyses from 1951 to 2014. These six regimes consist of cyclonic/anticyclonic oppositions between the Norwegian Sea and Russia (Scandinavian Blocking (SB) and Atlantic Trough (AT), Figures 1a and c), Greenland/Iceland and the Barents Sea (European Blocking (EB) and Scandinavian Trough (ST), Figures 1b and f), or Greenland and the North Sea (Greenland Blocking (GB) and Zonal (Zo), Figures 1d and e). These regimes are similar to six of the seven annual regimes identified in the North Atlantic region by Grams et al. (2017) and correspond to a combination between the winter and summer regimes identified by previous studies (Cassou et al., 2004; Grams et al., 2017; Guemas et al., 2010).

Similar anomaly patterns are observed with ERAI in the overlap period 1979-2014 (not shown). The inter-annual occurrence of the six regimes are consistent from one reanalysis to another (Figure 2). The correlation coefficient between the occurrence of regimes from the two overlapping datasets (20CR and ERAI) for the 1979-2014 period is generally higher than 0.8 (Figure 2). The high correlation between 20CR and ERAI suggests that (i) the regimes are rather robust and reproducible (ii) both datasets can produce such recurrent atmospheric configurations for this period. Therefore, the temporal occurrence of the regimes is not model-dependent for the 1979-2014 period.

Some regimes display some significant inter-annual trends over the 1951-2014 period, especially in summer (Figure 2). “Greenland Blocking” (GB) and “Scandinavian Blocking” (SB) show significant increase in temporal recurrence while “Atlantic Trough” (AT) shows a significant decline (Figure 2). These results suggest an increasing frequency of anticyclonic conditions over Greenland and the North Sea. During winter, the results show a negative inter-annual trend in the occurrence of GB. However, after low occurrences in the late 1980s and early 1990s, GB occurrences increase during the late 1990s. During the fall and spring seasons, the regimes frequencies do not show significant evolution over the study period.

3.2. Inter-annual temperature variability

The relevance of the weather regimes in explaining regional atmospheric temperature changes is assessed at low frequency timescale by calculating the inter-annual correlation between CTL and EXP datasets (Figure 3). The correlation is generally high during winter for the entire domain ($r = 0.6$) and the highest inter-annual correlations occur in northeastern

Canada, Scandinavia, Greenland, and Russia (Figure 3a). The other seasons show a lower domain averaged correlation (r = 0.4) than winter. The statistical significance of correlations is not reached in northeastern Canada in summer and fall. Near the North Pole, the correlations are low or insignificant in all seasons. Figure 3 shows that regions with high correlations generally change season-to-season with the exception of Labrador Sea or Norwegian Sea showing high correlations consistently throughout the year. This result indicates that the location and persistence of weather regimes partially explain the high-frequency variability of surface temperature in most parts of the study domain.

3.3. Decadal temperature evolution

Figures 4 and 5 show the trend of temperature in the Atlantic Arctic sector from 1951 to 2014 derived from CTL and EXP. The evolution of temperature for the CTL dataset varies in space and is dependent on the season (Figure 4). In winter and spring, strong atmospheric warming occurs between the North Pole and the Barents Sea, with temperature increasing by 1 to 2 degrees per decade, while the northeastern Canadian landmass experiences a cooling (Figure 4a-b). During summer, the largest increase is located between the Barents Sea and the Greenland Sea (Figure 4c). In fall the largest temperature increases is observed in the area close to the North Pole (> 85°N), while a cooling is observed in the Fram Strait (Figure 4d). Results of the EXP dataset show that the largest changes occur in winter, with significant temperature increases in the Norwegian-Greenland Seas, while northeastern Canada and the Labrador Sea experienced a cooling trend (Figure 5a). This thermal dipole is found in both CTL and EXP in winter and spring (Figures 4a-b and 5a-b). During the summer and fall,

similarities between the two datasets are less clear (Figures 4c-d and 5c-d). In summer, CTL shows a warming in northeastern Canada and the Barents Sea, but a cooling in the Greenland ice cap (Figure 4c)., while EXP depicts an opposite trend (Figure 5c).

Figure 6 shows the regions where the CTL temperature trend is related to EXP temperature trend (ratio of EXP to CTL). During winter, some regions of northeastern Canada (Labrador coast and Baffin Island) are characterized by a large percentage of cooling, while the North Atlantic Ocean (particularly the Norwegian-Greenland Seas) is affected by a large percentage of warming. In these regions, about 25% of the temperature trend can be explained by changes in the regime occurrences. These results are considered as robust since they are weakly dependent on the start/end points of the time series. Summer shows a relatively large percentage of warming in Norway, Iceland, and the seas surrounding Greenland (Figure 6c). In Norway up to 40% of the temperature warming is due to the regimes, but this estimation needs to be taken with caution, as this region shows results strongly dependent on the period used for the computation (Figure 6c). However, a large part of the domain shows robust results for both summer and winter seasons, especially in the Norwegian-Greenland Seas (Figure 6a and 6c), confirming a clear relationship between atmospheric circulation and low-frequency evolutions of temperature. In contrast, during spring and fall, the evolution of temperature attributed to changes in weather regime frequency is low (Figure 6b and 6d).

3.4. Regional temperature variability during summer and winter

Enhanced warming areas during summer or winter include Norway, Iceland, eastern Greenland, northeastern Canada and Spitsbergen (all display as black boxes in Figure 6c).

These lands show the same sign of temperature change in CTL and EXP during winter or summer (Figure 6a and 6c) and are used to study the co-variability between CTL and EXP at different timescales. Spring and fall are not considered further below, as EXP to CTL ratios are not robust (Figure 6b and 6d) and the trends of temperatures in EXP dataset are not significant at 95% confidence level (Figure 5b and 5d).

Winter temperature correlations between detrended CTL and EXP are high in the aforementioned five regions, especially in northeastern Canada ($r = 0.76$) and Norway ($r = 0.75$) (Figure 7). For example, the year 2010 was a very warm season in northeastern Canada (4°C above average), but a very cold period in Norway (2°C below average) and the EXP reconstruction replicates these anomalies. Co-variability at decadal timescales is also observed in northeastern Canada and Norway. Low temperatures occur in northeastern Canada in both datasets during the 1990s (Figure 7d) while in Norway, the same period is characterized by positive anomalies (Figure 7a). Hence, regime occurrence explains much temperature trend from 1951 to 2014 in Iceland (22%), Norway (25%), northeastern Canada (26%), and Greenland (27%).

During the summer season, the inter-annual variability of EXP is low compared to CTL in most of the studied areas (Figure 8). Compared to winter, the co-variability between EXP and CTL is low in northeastern Canada, Spitsbergen and Iceland ($r < 0.47$). The co-variability remains high in Norway ($r = 0.76$) and even increases in Greenland ($r = 0.64$). The ratio of EXP to CTL also shows lower values (< 15%) except for Norway (37%).

3.5. Physical mechanisms modulating intra-regimes temperature

This section analyses the anomalies of different climate variables that correspond to each regime to assess the physical mechanisms through which the weather regimes modulate intra-seasonal temperature variability.

Winter southerly winds (eastern side of a cyclone and western side of an anticyclone) are associated with warm anomalies, while northerly winds are associated with cold anomalies (Figure 9). Regions of intense warm anomalies are also associated with higher cloud water content in southern Greenland (Figures 9a and 10a), eastern Greenland (Figures 9b and 10b), northeastern Canada (Figures 9d and 10d) and Scandinavia (Figures 9e and 10e). The same regions are also associated with high downward IR (Figure 10).

In summer, regions showing the warmest temperature anomalies correspond to the center of high geopotential systems (Figure 11). These regions are also generally associated with lower cloud cover ratio and higher downward SR (Figure 12). The regime GB is an exception with high Z500 and high temperatures in Greenland not associated with high downward SR (Figures 11d and 12d). Warm anomalies are also associated with south/southeasterly winds in the North Atlantic Ocean, especially in the Labrador Sea (Figure 11d), the Norwegian Sea (Figure 11a and 11d), and the Barents Sea (Figure 11b). However, the warm anomalies in these regions have a lower magnitude than the anomalies close to the center of anticyclonic systems (Figure 11).

Taken together, our results suggest that weather regimes are relevant in controlling the 1951-2014 variability of atmospheric temperature during winter and summer within the Atlantic-Arctic region. Year-to-year variability of air temperature may be strongly driven by weather regimes, and thus changes in the atmospheric circulation, especially on both sides of the

Atlantic Ocean. Weather regimes were also found to explain a non-negligible fraction (22-27%) of the evolution of winter temperature from 1951 to 2014 in the Norwegian-Greenland Seas and northeastern Canada. In summer, the influence of weather regimes on the overall warming in Norwegian-Greenland Seas is lower (12-15%), but the weather regime influence is enhanced in Norway (37%).

4. Discussion

4.1. Relationship between occurrence of weather regimes and temperature variability at different timescales

The temperature variability in the Atlantic Arctic is partially linked to a change in occurrence of weather regimes. Generally, the relationship between such regimes and temperature is strong at inter-annual timescale (Figures 3, 7 and 8), but also at decadal timescale for specific locations in winter and summer (Figures 6, 7 and 8).

4.1.1. Impact of weather regimes on inter-annual temperature variability

During winter, temperature anomalies are well constrained by the weather regimes Z500 anomalies (Figure 9) and are mostly modulated by the advection of warm and cold air masses as well as the downward IR depending on water vapor (Figures 9 and 10). The two datasets (EXP and CTL) are well correlated at high-frequency timescales particularly in northeastern Canada and Norway (Figures 3a and 7) suggesting that concurrent regime-thermal occurrences exist at this time scale. For example, the regime Zonal (Zo) is characterized by low-pressure anomalies centered over Greenland and high-pressure anomalies over western

Europe, which causes warm temperatures over Scandinavia, but cold conditions over northeastern Canada and Greenland (Figure 9e). During regime Zo, the wind advects warm air masses to a large area of the North-Atlantic Ocean and northern Europe (Figure 9e). In Scandinavia, the warm anomalies are reinforced by downward IR due to water vapor increases (Figure 10e) brought by the southwesterly winds. During the early 1990s Zo was prevalent in winter (Figure 2), which forced Norway to experience anomalously warm temperatures while cold conditions persisted in northeastern Canada (Figure 7a and 7d). The regime Greenland Blocking (GB) with a mean frequency of 15 occurrences per winter (1951-2014) occurred significantly more during the 2010 winter (60 occurrences) (Figure 2). GB corresponds to cold anomalies in the region east of Greenland and warm anomalies in the western part of the North-Atlantic basin (Figure 9d). The winter of 2010 was therefore associated with cold anomalies in Norway (Figure 7a) but warm anomalies in northeastern Canada (Figure 7d). Similarly, to the mechanism occurring in Scandinavia during a regime Zo, the warm anomalies observed in northeastern Canada during a regime GB are reinforced by high downward IR (Figure 10d). Atmospheric circulation within the region between Spitsbergen, Iceland and eastern Greenland, appears to have a lower impact on temperature variability at low frequency timescales (Figures 3a and 7). The regions of cold and warm anomalies found in this study are in accordance with Papritz & Grams (2018), who pointed out more cold outbreaks in the Norwegian Sea during the regime GB and in southern Greenland during the regime Zo. Our results also corroborates the study of Yao et al., (2018) identifying strong warm anomalies increased by downward IR over the western part of high pressure systems.

In summer, the results suggest a lower impact of atmospheric circulation on inter-annual temperature variability over the area (Figures 3c and 8) which may be due to weaker Z500 anomalies (Figures 9 and 11). The co-variability remains strong in Norway and coastal Greenland (Figures 3c and 8). Norway is associated with strong regime-thermal anomalies (Figure 11) likely due to strong downward SR and cloud cover anomalies (Figure 12). On the Greenland ice cap, the association between high-pressure, high-downward SR and high-temperature anomalies is less clear (Figures 11 and 12). The high-pressure conditions over Greenland (regime GB) are associated with warm temperature anomalies (Figure 11d), but not with low cloud cover nor high downward SR anomalies (Figure 12d). The low co-variability between high pressure conditions and low cloud cover is likely due to a low-level inversion layer. The high pressure on Greenland may favor low level clouds and an increase of downward IR and temperature. The summer downward IR are not analyzed in our study, but the association between high downward IR and high Z500 anomalies in Greenland was recently shown (Ding et al. 2017). In other regions such as the Norwegian Sea (Figure 11a-b), the Barents Sea (Figure 11b) and the Labrador Sea (Figure 11d), the advection of meridional air is likely the cause of warm anomalies. In Iceland, the highest warm anomalies occur during the regimes SB and EB, associated with southerly winds (Figure 11a-b). The anomalies of cloud cover and downward SR are not significant during these regimes (Figure 11a-b), suggesting that the meridional winds play an important role in the warm anomalies in Iceland. Similarly, Matthews et al., (2015) show an association between anticyclonic conditions in the Norwegian Sea and highest glacier melt in Iceland, due to a meridional advection of latent heat flux and an enhancement of longwave IR. Our overall results

corroborate Guemas et al. (2010) showing an association between Scandinavian Blocking and warm temperature driven by different processes. In Scandinavia the dominant process is the downward SR while in the North Atlantic Ocean the advection of heat flux and downward IR are more prominent.

4.1.2. Impact of weather regimes on temperature trends

During winter, the dipole in the overall temperature trend between northeastern Canada and the Norwegian-Greenland Seas (Figure 6a) is likely due to GB occurrence decreases (Figure 2). In northeastern Canada, GB is the only regime associated with warm anomalies (Figure 9), suggesting that the long-term cooling in this region are linked to the decline of GB frequency. The temperature trend in these regions is reversed since the 1990's (Figure 7a and 7d) likely due to a recovery of GB frequency (Figure 2). These results suggest that the long-term winter warming from anthropogenic origins is not occurring to the same effect in the entire domain as the variability of GB frequency affects the decadal variability of temperature in northeastern Canada and the Norwegian-Greenland Seas region. In Spitsbergen, a strong warm anomaly starting in the early 2000s occurred (Figure 7e). Since then, the CTL temperature is consistently above the EXP temperature in this region, showing that this warming is probably not linked to atmospheric circulation.

In summer the impact of weather regimes on the warming trend is mostly observed in Norway (Figures 6c and 8a). The warming observed in this region (Figure 4c) is explained for a large part by changes in regime frequency (Figures 6c and 8a). This is in accordance with regime Scandinavian Blocking (SB), which occurred more frequently in recent decades

(Figure 2) and is characterized by warm anomalies, low cloud cover anomalies and high shortwave radiations anomalies over Norway (Figure 11a and 12a). There are competing effects with regime GB which is also more frequent recently during the summer but associated with cold anomalies over Norway (Figure 11d). However, GB has lower influence on Norway because GB frequency is lower on average and its occurrence increased less from 1951 to 2014 (Figure 2). Moreover, regime European Blocking (EB) is also more frequent throughout the period and is associated with warm anomalies over Norway (Figure 11b). In other regions within the Norwegian-Greenland Seas area, the increase of Blocking regimes frequency played a minor role in the warming (15%). Previous works indicate that warmer conditions, especially in Greenland, are because of the persistence of anticyclonic conditions during summer (Bezeau et al., 2015; Fettweis et al., 2011; McLeod & Mote, 2016; Mioduszewski et al., 2016). We completed these studies by showing that part of the warming is due to an increase of anticyclonic conditions in a large area of Norwegian-Greenland Sees and surrounding lands. We suggested different processes associating Blocking conditions and warming. In the North-Atlantic-Ocean (Labrador-Greenland-Norwegian Seas) the more frequent anticyclonic recurrences may have enhanced the meridional advection of heat flux and warming. In Norway, the increase of Scandinavian Blocking frequency probably increased the meridional winds and downward SR. These two combined processes likely enhanced the warming.

4.2. Relevance of weather regimes in the Atlantic-Arctic region

4.2.1. Causal relationships between anticyclonic conditions and warming

Previous studies have shown that the Arctic warm temperature and ice melt increase could have caused the persistence of anticyclonic conditions instead of being a consequence (Balmaseda et al., 2010; Bezeau et al., 2015; Proshutinsky et al., 2015). Balmaseda et al., (2010) show that lower sea ice extent promotes more heat flux which could favor higher pressure. Bezeau et al., (2015) described the following feedback loop: increasing temperature enhances Z500; enhanced Z500 favors more downward IR/ meridional wind; more downward IR/meridional wind decreases albedo; decreased albedo finally increases temperature. Our study shows a strong link between anticyclonic conditions and warm temperature during summer in Norway (Figure 3c, 6c and 8a), but determining whether warm temperature or anticyclonic system is the first order remains a challenging task. By nudging modeled atmospheric circulation fields to observations, Ding et al. (2017) showed that anomalously high pressure over Greenland and Iceland, significantly contributed to the warming observed in summer in Greenland and northeastern Canada. Our results partially corroborate this study, with an increase of regime GB frequency (Figure 2) favoring warmer temperature conditions in coastal (Figure 6c). However, the trend ratio of EXP to CTL shows that less than 12% of the warming in Greenland eastern coastal areas and northeastern Canada can be explained by the regimes (Figure 8c-d). In Norway, the strong summer warming in recent decades correlates well with an increase of SB and EB regimes frequencies. These regimes are associated with meridional winds, low cloud cover and high shortwave radiation in Scandinavia, hereby suggesting an amplifying process between high pressure and high temperature there.

The strong summer ice melt in Barents sea is also known to increase high pressure anomalies in the Siberian region in winter (Crasemann et al., 2017), creating a positive feedback through advections of heat flux from the south (Figure 9b). Our study clearly shows that increasing temperature anomalies in the European Arctic in winter is at least partially caused by variability in weather regimes occurrences. First, the GB regime is affected by a long-term decrease in frequency (Figure 2) not likely linked to sea ice retreat. Second, the regions of northeastern Canada and Norway are located far from Greenland and the temperature in these regions are unlikely to cause a pressure system change centered on Greenland. It is therefore clear that the lower frequency high-pressure systems on Greenland have an impact on the temperature dipole between warming in the Atlantic Ocean and cooling in northeastern Canada in winter. Since the 1990s, sea ice melt can be the cause of the recent GB frequency recovery, which largely contributed to the recent warming in northeastern Canada (Figure 7d). There, GB is associated with southerly wind anomalies and increased downward IR (Figures 9d and 10d).

4.2.2. Intrinsic change of weather regime conditions

The weather regimes drive the thermal dipole between the Norwegian-Greanland Seas and northeastern Canada in winter. However, in Spitsbergen, the change of weather regimes accounts for a small part (11%) in the anomalously high warming in recent decades (Figures 6a and 7e). The regime contribution to the temperature trend is low compared to Norway or northeastern Canada, which can be attributed to a very low inter-regime variability in terms of atmospheric water content and downward IR anomalies (Figure 10). The low contribution

of atmospheric circulation in the Spitsbergen warming seems to be in contradiction with previous studies stating that European Blocking is associated with high temperature in this region, due to advections of wet air increasing downward IR (B. Luo et al., 2017; Rinke et al., 2017; Yao et al., 2018). Dahlke & Maturilli, (2017) estimate that 22% of the warming in Ny Ålesund (Spitsbergen) relates to an increase of European Blocking. Here, we find an increase of the regime EB (Figure 2), but this increase is not statistically significant (Figure 2) and has a low impact on warming in Spitsbergen (Figure 7e), likely due to our longer study period. The hypothesis of a discrepancy due to a different study period length is partly confirmed by our examination of the EXP to CTL ratio linear trends over a similar period (1996-2014). We show a nearly 15% contribution of regime patterns to the warming between 1996 and 2014 in Spitsbergen.

Isaksen et al. (2016) also show that 25% of the warming in Spitsbergen can be attributed to a shift in atmospheric circulation, but the rest is attributed to larger ice-free areas in the Barents Sea modifying air mass characteristics. These authors show a strong warming during anticyclonic condition anomalies on Greenland due to advection of air from the warming Barents Sea. Isaksen et al. (2016) suggest that temperature anomalies associated with specific meteorological systems can change in time. In our study, the mean temperature for each weather regime, used to calculate the EXP dataset, is based on the 1951 to 2014 record and do not take into consideration the intrinsic decadal change of temperature conditions that may correspond to each regime.

The surface intra-regime temperature trend from 1951 to 2014 in winter was calculated for each grid point. The daily temperatures corresponding to each regime have been averaged for

each year and the linear regression coefficient of these yearly data have been calculated, determining the evolution of temperature per decade (Figure 13). The regressive correlation shows a warming in the Barents Sea and close to the North-Pole consistently for each regime, suggesting that the warming is largely independent of regimes (Figure 13). For GB, the warming is stronger in Spitsbergen and also occurs in the Atlantic Ocean, possibly because of advective effects associated with northerly wind anomalies originating from the Barents Sea (Figure 13d). The intrinsic warming to GB suggests that warming in Spitsbergen and the Norwegian-Greenland Seas come from two different processes. First, the decrease of GB frequency reduced advections of cold air masses from the north and second, the cold air masses themselves have been warming recently. The same mechanism is likely to occur during regimes ST and SB. ST is associated with an increase of temperature in northern Greenland (Figure 13f), likely due to similar advective effects from the Barents Sea (Figure 9f). The same mechanism may explain the association between regime SB and warming in northern Scandinavia (Figures 9a and 13a). According to Isaksen (2016), the heat loss from newly open water in the Barents Sea is more likely to occur under low-pressure systems, i.e. typically the conditions associated with GB, ST and SB. This energy is then advected to other regions, depending on the direction of the wind. Similarly, the interannual correlation between warm temperature in eastern Greenland and low sea-ice volume during cyclonic conditions in the Barents Sea was shown by Ogi et al., (2016).

The evolution of the surface temperature from 1951 to 2014 (Figure 13) suggests that the cooling observed in northeastern Canada is driven by different processes. Generally, in Labrador, the temperature associated with each regime does not significantly change (white

areas in Figure 13). The lack of significant temperature change intrinsic to each regime supports the fact that cooling in Labrador is associated with weather regime occurrence change (Figure 6a). A second cause can involve a change in sea surface temperature near the southern Greenland coast. The cooling in northeastern Canada is higher for the regime SB (Figure 13a), concomitant with southeasterly wind anomalies originating from southern Greenland (Figure 9a). In recent decades, cooling sea surface temperature has been observed close to the southern Greenland coast due to a surplus of low-density freshwater melt from the Greenland ice caps (Josey et al., 2018). Such cooling is transferred to the surface temperature (Figure 4a) and the southeasterly winds associated with high pressure over the Norwegian Sea (Figure 9a) may favor advection towards northeastern Canada.

4.2.3. Seasonality of the links between temperature and weather regimes

Temperature anomalies are less significantly linked to weather regimes during the fall and spring seasons. The lack of significance suggests the mechanisms involved during the coldest and warmest months cannot be replicated during fall and spring. The advective processes and downward IR are the only dominant processes driving temperature variability in winter, while shortwave SR also plays a role in the summer temperature variability. During fall and spring there is likely a mix of these processes, interfering with the signals driven by regime frequency and change. At the scale of decadal temperature, the change patterns during spring seem to follow the same trend as those during winter (Figures 4a-b and 5a-b). This suggests that the dominant processes explaining the temperature variability in winter are attenuated in

spring. This is further corroborated by our analysis using the night time period only, where no significant relationships are found (not shown).

5. Conclusion

This study highlighted the drivers of atmospheric circulation on temperature variations in the Atlantic Arctic from 1951 to 2014 during a period of global warming within the study region. The weather regimes, founded on the recurrence of the meteorological systems, are based on daily Z500 anomalies. This method has been widely used in western Europe and was tested here in the Atlantic Arctic region. Six regimes have been defined and the pattern calculated from ERAI and 20CR re-analyses are consistent for a 35-year overlap period. The fraction of temperature trends due to changes in the weather regimes were calculated to assess their contribution on the region recent warming. The major findings are summarized as follows:

1. We found a strong link between weather regimes and temperature variability at different timescales in winter. Northeastern Canada and Norway are especially affected by the Greenland Blocking and zonal regimes. These regimes are characterized by a change in pressure systems centered over Greenland, modulating the advection of warm and cold air masses over these regions. This process can be amplified by the advection of air moisture modulating the amount of downward infrared radiation. We found around 25% of the warming and cooling observed respectively in the Norwegian-Greenland Seas and northeastern Canada attributed to a long-term decrease of high-pressure systems frequencies over Greenland.

2. The intrinsic temperature trend corresponding to each regime in winter suggests that some weather regimes can act as a vector to transport air masses from regions affected by a temperature change in winter. This process is another possible cause of northeastern Canada cooling, mainly observed for periods corresponding to high pressure conditions over the Norwegian Sea (regime SB). The air masses brought by these high-pressure conditions are cooling in recent decades because of a colder sea surface temperature due to Greenland freshwater ice-melt. In Spitsbergen, northern Scandinavia, and northern Greenland, a winter warming amplification may be explained by warmer air masses from the Barents Sea, an area subjected to enhanced warming due to sea ice loss.
3. In summer, 15% of the warming observed in the Norwegian-Greenland Seas and surrounding lands, including Iceland, Spitsbergen and eastern Greenland, is attributed to more meridional winds due to the persistence of anticyclonic systems. The contribution of weather regimes to the warming is reinforced in Norway (37%) due to a combination effect of enhanced meridional winds and downward shortwave radiation associated with the Scandinavian Blocking.

For the future analyses, our results could be complemented by including more analyses on heat-fluxes and radiations. Intra-regime variability of geopotential height and how it affects heat fluxes, radiations and temperature should also be investigated. Moreover, applying the same method with a domain centered on other regions of the Arctic may help investigate the impact of atmospheric circulation on temperature changes in North America or the Pacific Ocean longitudes. Future investigations should especially focus on temperature variability

linkages during spring and autumn, as both of these seasons show insignificant linkages in this study, while they correspond to key periods of the glacio-hydrological process. The method used in this study could also be applied to the future climate simulations with the different RCP scenarios from CMIP5. These future investigations could use downscaling data to increase the robustness of the results and especially take advantage of recent improvement of regional simulations in the Arctic including the Arctic Coordinated Regional Climate Downscaling Experiment (Arctic-CORDEX). These studies will help to reduce uncertainty in the regional temperature predictions and their impacts on the cryosphere.

Acknowledgments

National Oceanic & Atmospheric administration (NOAA) website furnished 20thCR reanalysis V2 and European Centre for Medium-Range Weather Forecasts (ECMWF) furnished ERAI reanalysis. Calculations were performed using high-performance computing (HPC) resources from DSI-CCUB, Université de Bourgogne. We also thank the anonymous reviewers for their comments to improve the content of this manuscript.

References

Alvarez-Castro, M. C., Faranda, D., & Yiou, P. (2018). Atmospheric Dynamics Leading to West European Summer Hot Temperatures Since 1851. *Complexity*, *2018*, 1-10. https://doi.org/10.1155/2018/2494509

Balmaseda, M. A., Ferranti, L., Molteni, F., & Palmer, T. N. (2010). Impact of 2007 and 2008 Arctic ice anomalies on the atmospheric circulation: Implications for long-range predictions. *Quarterly Journal of the Royal Meteorological Society*, *136*(652), 1655-1664. https://doi.org/10.1002/qj.661

Bekryaev, R. V., Polyakov, I. V., & Alexeev, V. A. (2010). Role of Polar Amplification in Long-Term Surface Air Temperature Variations and Modern Arctic Warming. *Journal of Climate*, *23*(14), 3888-3906. https://doi.org/10.1175/2010JCLI3297.1

Bezeau, P., Sharp, M., & Gascon, G. (2015). Variability in summer anticyclonic circulation over the Canadian Arctic Archipelago and west Greenland in the late 20th/early 21st centuries and its effect on glacier mass balance. *International Journal of Climatology*, *35*(4), 540-557. https://doi.org/10.1002/joc.4000

Cassou, C., Terray, L., Hurrell, J. W., & Deser, C. (2004). North Atlantic winter climate regimes: Spatial asymmetry, stationarity with time, and oceanic forcing. *Journal of Climate*, *17*(5), 1055-1068. https://doi.org/10.1175/1520-0442(2004)017<1055:NAWCRS>2.0.CO;2

Cassou, C., Terray, L., & Phillips, A. S. (2005). Tropical Atlantic influence on European heat waves. *Journal of Climate*, *18*(15), 2805-2811. https://doi.org/10.1175/JCLI3506.1

Compo, G. P., Whitaker, J. S., Sardeshmukh, P. D., Matsui, N., Allan, R. J., Yin, X., et al. (2011). The twentieth century reanalysis project. *Quarterly Journal of the Royal Meteorological Society*, *137*(654), 1-28. https://doi.org/10.1002/qj.776

Crasemann, B., Handorf, D., Jaiser, R., Dethloff, K., Nakamura, T., Ukita, J., & Yamazaki, K. (2017). Can preferred atmospheric circulation patterns over the North-Atlantic-Eurasian region be associated with arctic sea ice loss? *Polar Science*, *14*, 9-20. https://doi.org/10.1016/j.polar.2017.09.002

Dahlke, S., & Maturilli, M. (2017). Contribution of Atmospheric Advection to the Amplified Winter Warming in the Arctic North Atlantic Region. *Advances in Meteorology*, *2017*, 1-8. https://doi.org/10.1155/2017/4928620

Dee, D. P., Uppala, S. M., Simmons, A. J., Berrisford, P., Poli, P., Kobayashi, S., et al. (2011). The ERA-Interim reanalysis: configuration and performance of the data assimilation system. *Quarterly Journal of the Royal Meteorological Society*, *137*(656), 553-597. https://doi.org/10.1002/qj.828

Ding, Q., Schweiger, A., L'Heureux, M., Battisti, D. S., Po-Chedley, S., Johnson, N. C., et al. (2017). Influence of high-latitude atmospheric circulation changes on summertime

Arctic sea ice. *Nature Climate Change*, *7*(4), 289-295. https://doi.org/10.1038/nclimate3241

Fettweis, X., Mabille, G., Erpicum, M., Nicolay, S., & den Broeke, M. V. (2011). The 1958–2009 Greenland ice sheet surface melt and the mid-tropospheric atmospheric circulation. *Climate Dynamics*, *36*(1-2), 139-159. https://doi.org/10.1007/s00382-010-0772-8

Fleig, A. K., Tallaksen, L. M., James, P., Hisdal, H., & Stahl, K. (2015). Attribution of European precipitation and temperature trends to changes in synoptic circulation. *Hydrology and Earth System Sciences*, *19*(7), 3093-3107. https://doi.org/10.5194/hess-19-3093-2015

Gardner, A. S., Moholdt, G., Wouters, B., Wolken, G. J., Burgess, D. O., Sharp, M. J., et al. (2011). Sharply increased mass loss from glaciers and ice caps in the Canadian Arctic Archipelago. *Nature*, *473*(7347), 357-360. https://doi.org/10.1038/nature10089

Gerlitz, L., Steirou, E., Schneider, C., Moron, V., Vorogushyn, S., & Merz, B. (2018). Variability of the Cold Season Climate in Central Asia. Part I: Weather Types and Their Tropical and Extratropical Drivers. *Journal of Climate*, *31*(18), 7185-7207. https://doi.org/10.1175/JCLI-D-17-0715.1

Grams, C. M., Beerli, R., Pfenninger, S., Staffell, I., & Wernli, H. (2017). Balancing Europe's wind-power output through spatial deployment informed by weather regimes. *Nature Climate Change*, *7*(8), 557-562. https://doi.org/10.1038/nclimate3338

Guemas, V., Salas-Mélia, D., Kageyama, M., Giordani, H., Voldoire, A., & Sanchez-Gomez, E. (2010). Summer interactions between weather regimes and surface ocean in the North-Atlantic region. *Climate Dynamics*, *34*(4), 527-546. https://doi.org/10.1007/s00382-008-0491-6

Hanna, E., Jones, J. M., Cappelen, J., Mernild, S. H., Wood, L., Steffen, K., & Huybrechts, P. (2013). The influence of North Atlantic atmospheric and oceanic forcing effects on 1900-2010 Greenland summer climate and ice melt/runoff. *International Journal of Climatology*, *33*(4), 862-880. https://doi.org/10.1002/joc.3475

Hanna, E., Hall, R. J., Cropper, T. E., Ballinger, T. J., Wake, L., Mote, T., & Cappelen, J. (2018). Greenland blocking index daily series 1851-2015: Analysis of changes in

extremes and links with North Atlantic and UK climate variability and change. *International Journal of Climatology*, *38*(9), 3546-3564. https://doi.org/10.1002/joc.5516

Holland, M. M., & Bitz, C. M. (2003). Polar amplification of climate change in coupled models. *Climate Dynamics*, *21*(3-4), 221-232. https://doi.org/10.1007/s00382-003-0332-6

Hurrell, J. W., & Deser, C. (2010). North Atlantic climate variability: The role of the North Atlantic Oscillation. *Journal of Marine Systems*, *79*(3-4), 231-244. https://doi.org/10.1016/j.jmarsys.2009.11.002

Isaksen, K., Nordli, Ø., Førland, E. J., Aupikasza, E., Eastwood, S., & Niedzwiedz, T. (2016). Recent warming on Spitsbergen-Influence of atmospheric circulation and sea ice cover. *Journal of Geophysical Research: Atmospheres*, *121*(20), 11,913-11,931. https://doi.org/10.1002/2016JD025606

James, T. D., Murray, T., Barrand, N. E., Sykes, H. J., Fox, A. J., & King, M. A. (2012). Observations of enhanced thinning in the upper reaches of Svalbard glaciers. *The Cryosphere*, *6*(6), 1369-1381. https://doi.org/10.5194/tc-6-1369-2012

Josey, S. A., Hirschi, J. J.-M., Sinha, B., Duchez, A., Grist, J. P., & Marsh, R. (2018). The Recent Atlantic Cold Anomaly: Causes, Consequences, and Related Phenomena. *Annual Review of Marine Science*, *10*(1), 475-501. https://doi.org/10.1146/annurev-marine-121916-063102

Kaser, G., Cogley, J. G., Dyurgerov, M. B., Meier, M. F., & Ohmura, A. (2006). Mass balance of glaciers and ice caps: Consensus estimates for 1961-2004. *Geophysical Research Letters*, *33*(19). https://doi.org/10.1029/2006GL027511

Kohler, J., James, T. D., Murray, T., Nuth, C., Brandt, O., Barrand, N. E., et al. (2007). Acceleration in thinning rate on western Svalbard glaciers. *Geophysical Research Letters*, *34*(18). https://doi.org/10.1029/2007GL030681

Lang, A., Yang, S., & Kaas, E. (2017). Sea ice thickness and recent Arctic warming. *Geophysical Research Letters*, *44*(1), 409-418. https://doi.org/10.1002/2016GL071274

Luo, B., Luo, D., Wu, L., Zhong, L., & Simmonds, I. (2017). Atmospheric circulation patterns which promote winter Arctic sea ice decline. *Environmental Research Letters*, *12*(5), 054017. https://doi.org/10.1088/1748-9326/aa69d0

Luo, D., Xiao, Y., Yao, Y., Dai, A., Simmonds, I., & Franzke, C. L. E. (2016). Impact of Ural Blocking on Winter Warm Arctic–Cold Eurasian Anomalies. Part I: Blocking-Induced Amplification. *Journal of Climate*, *29*(11), 3925-3947. https://doi.org/10.1175/JCLI-D-15-0611.1

Mahajan, S., Zhang, R., & Delworth, T. L. (2011). Impact of the Atlantic Meridional Overturning Circulation (AMOC) on Arctic Surface Air Temperature and Sea Ice Variability. *Journal of Climate*, *24*(24), 6573-6581. https://doi.org/10.1175/2011JCLI4002.1

Matthews, T., Hodgkins, R., Guðmundsson, S., Pálsson, F., & Björnsson, H. (2015). Inter-decadal variability in potential glacier surface melt energy at Vestari Hagafellsjökull (Langjökull, Iceland) and the role of synoptic circulation: MELT ENERGY AND SYNOPTIC CIRCULATION AT VESTARI HAGAFELLSJÖKULL. *International Journal of Climatology*, *35*(10), 3041-3057. https://doi.org/10.1002/joc.4191

McLeod, J. T., & Mote, T. L. (2016). Linking interannual variability in extreme Greenland blocking episodes to the recent increase in summer melting across the Greenland ice sheet: EXTREME GREENLAND BLOCKING AND SUMMER MELTING ACROSS THE GREENLAND ICE SHEET. *International Journal of Climatology*, *36*(3), 1484-1499. https://doi.org/10.1002/joc.4440

McLeod, J. T., Ballinger, T. J., & Mote, T. L. (2018). Assessing the climatic and environmental impacts of mid-tropospheric anticyclones over Alaska: CLIMATIC IMPACTS OF MID-TROPOSPHERIC ANTICYCLONES OVER ALASKA. *International Journal of Climatology*, *38*(1), 351-364. https://doi.org/10.1002/joc.5180

Meier, M. F., Dyurgerov, M. B., Rick, U. K., O'Neel, S., Pfeffer, W. T., Anderson, R. S., et al. (2007). Glaciers Dominate Eustatic Sea-Level Rise in the 21st Century. *Science*, *317*(5841), 1064-1067. https://doi.org/10.1126/science.1143906

Mernild, S. H., Liston, G. E., Hiemstra, C. A., & Christensen, J. H. (2010). Greenland Ice Sheet Surface Mass-Balance Modeling in a 131-Yr Perspective, 1950-2080. *Journal of Hydrometeorology*, *11*(1), 3-25. https://doi.org/10.1175/2009JHM1140.1

Michelangeli, P.-A., Vautard, R., & Legras, B. (1995). Weather Regimes: Recurrence and Quasi Stationarity. *Journal of the Atmospheric Sciences*, *52*(8), 1237-1256. https://doi.org/10.1175/1520-0469(1995)052<1237:WRRAQS>2.0.CO;2

Mioduszewski, J. R., Rennermalm, A. K., Hammann, A., Tedesco, M., Noble, E. U., Stroeve, J. C., & Mote, T. L. (2016). Atmospheric drivers of Greenland surface melt revealed by self-organizing maps: ATMOSPHERIC FORCING OF GREENLAND MELT. *Journal of Geophysical Research: Atmospheres*, *121*(10), 5095-5114. https://doi.org/10.1002/2015JD024550

Murawski, A., Vorogushyn, S., Bürger, G., Gerlitz, L., & Merz, B. (2018). Do Changing Weather Types Explain Observed Climatic Trends in the Rhine Basin? An Analysis of Within- and Between-Type Changes. *Journal of Geophysical Research: Atmospheres*, *123*(3), 1562-1584. https://doi.org/10.1002/2017JD026654

Nilsen, I. B., Stagge, J. H., & Tallaksen, L. M. (2017). A probabilistic approach for attributing temperature changes to synoptic type frequency: Probabilistic approach to attribute temperature changes. *International Journal of Climatology*, *37*(6), 2990-3002. https://doi.org/10.1002/joc.4894

Ogawa, F., Keenlyside, N., Gao, Y., Koenigk, T., Yang, S., Suo, L., et al. (2018). Evaluating Impacts of Recent Arctic Sea Ice Loss on the Northern Hemisphere Winter Climate Change. *Geophysical Research Letters*, *45*(7), 3255-3263. https://doi.org/10.1002/2017GL076502

Ogi, M., Rysgaard, S., & Barber, D. G. (2016). The influence of winter and summer atmospheric circulation on the variability of temperature and sea ice around Greenland. *Tellus A: Dynamic Meteorology and Oceanography*, *68*(1), 31971. https://doi.org/10.3402/tellusa.v68.31971

Oudar, T., Sanchez-Gomez, E., Chauvin, F., Cattiaux, J., Terray, L., & Cassou, C. (2017). Respective roles of direct GHG radiative forcing and induced Arctic sea ice loss on

the Northern Hemisphere atmospheric circulation. *Climate Dynamics*, *49*(11-12), 3693-3713. https://doi.org/10.1007/s00382-017-3541-0

Overland, J. E., & Wang, M. (2016). Recent Extreme Arctic Temperatures are due to a Split Polar Vortex. *Journal of Climate*, *29*(15), 5609-5616. https://doi.org/10.1175/JCLI-D-16-0320.1

Overland, J. E., Francis, J. A., Hanna, E., & Wang, M. (2012). The recent shift in early summer Arctic atmospheric circulation. *Geophysical Research Letters*, *39*(19). https://doi.org/10.1029/2012GL053268

Papritz, L., & Grams, C. M. (2018). Linking Low-Frequency Large-Scale Circulation Patterns to Cold Air Outbreak Formation in the Northeastern North Atlantic. *Geophysical Research Letters*, *45*(5), 2542-2553. https://doi.org/10.1002/2017GL076921

Pithan, F., & Mauritsen, T. (2014). Arctic amplification dominated by temperature feedbacks in contemporary climate models. *Nature Geoscience*, *7*(3), 181-184. https://doi.org/10.1038/ngeo2071

Pohl, B., & Fauchereau, N. (2012). The Southern Annular Mode Seen through Weather Regimes. *Journal of Climate*, *25*(9), 3336-3354. https://doi.org/10.1175/JCLI-D-11-00160.1

Proshutinsky, A., Dukhovskoy, D., Timmermans, M.-L., Krishfield, R., & Bamber, J. L. (2015). Arctic circulation regimes. *Philosophical Transactions of the Royal Society A: Mathematical, Physical and Engineering Sciences*, *373*(2052), 20140160. https://doi.org/10.1098/rsta.2014.0160

Raymond, F., Ullmann, A., Camberlin, P., Oueslati, B., & Drobinski, P. (2018). Atmospheric conditions and weather regimes associated with extreme winter dry spells over the Mediterranean basin. *Climate Dynamics*, *50*(11-12), 4437-4453. https://doi.org/10.1007/s00382-017-3884-6

Rignot, E., Velicogna, I., van den Broeke, M. R., Monaghan, A., & Lenaerts, J. T. M. (2011). Acceleration of the contribution of the Greenland and Antarctic ice sheets to sea level rise. *Geophysical Research Letters*, *38*(5). https://doi.org/10.1029/2011GL046583

Rinke, A., Maturilli, M., Graham, R. M., Matthes, H., Handorf, D., Cohen, L., et al. (2017). Extreme cyclone events in the Arctic: Wintertime variability and trends. *Environmental Research Letters*, *12*(9), 094006. https://doi.org/10.1088/1748-9326/aa7def

Sasgen, I., van den Broeke, M., Bamber, J. L., Rignot, E., Sørensen, L. S., Wouters, B., et al. (2012). Timing and origin of recent regional ice-mass loss in Greenland. *Earth and Planetary Science Letters*, *333-334*, 293-303. https://doi.org/10.1016/j.epsl.2012.03.033

Screen, J. A., & Simmonds, I. (2010). The central role of diminishing sea ice in recent Arctic temperature amplification. *Nature*, *464*(7293), 1334-1337. https://doi.org/10.1038/nature09051

Sun, L., Allured, D., Hoerling, M., Smith, L., Perlwitz, J., Murray, D., & Eischeid, J. (2018). Drivers of 2016 record Arctic warmth assessed using climate simulations subjected to Factual and Counterfactual forcing. *Weather and Climate Extremes*, *19*, 1-9. https://doi.org/10.1016/j.wace.2017.11.001

Vigaud, N., Robertson, A. W., & Tippett, M. K. (2018). Predictability of Recurrent Weather Regimes over North America during Winter from Submonthly Reforecasts. *Monthly Weather Review*, *146*(8), 2559-2577. https://doi.org/10.1175/MWR-D-18-0058.1

Yao, Y., Luo, D., & Zhong, L. (2018). Effects of Northern Hemisphere Atmospheric Blocking on Arctic Sea Ice Decline in Winter at Weekly Time Scales. *Atmosphere*, *9*(9), 331. https://doi.org/10.3390/atmos9090331

Yiou, P., & Nogaj, M. (2004). Extreme climatic events and weather regimes over the North Atlantic: When and where? *Geophysical Research Letters*, *31*(7). https://doi.org/10.1029/2003GL019119

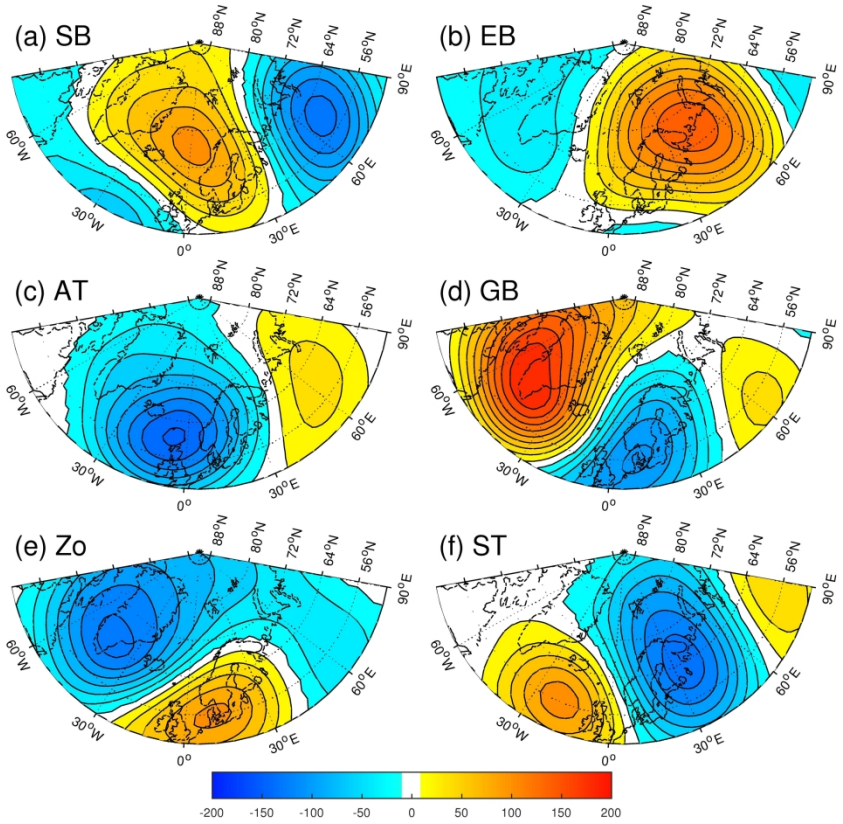

Figure 1. The six Atlantic-Arctic weather regimes examined in this study. For each regime (a to f) the spatial average geopotential height anomalies at 500 hPa are shown (Interval 20m). All anomalies are significant at the 95% confidence level according to t-test.

261x235mm (300 x 300 DPI)

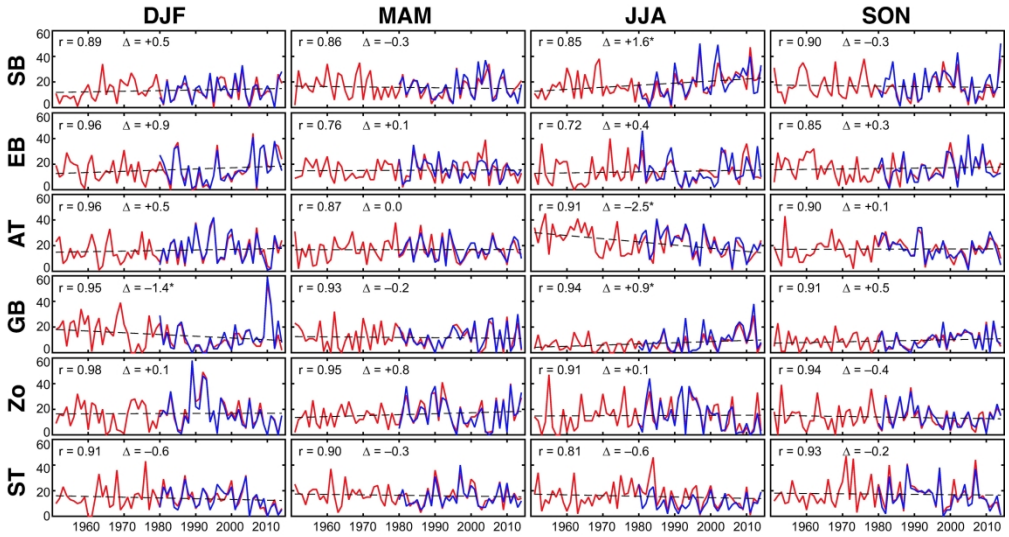

Figure 2. Number of seasonal occurrences of regimes according to 20CR over the period 1951-2014 (in red),and ERAI over the period 1979-2014 (in blue). The trend of the 20CR regimes frequency is shown as a dashed line, labeled by the evolution of frequency per decade (Δ) and followed by a star when significant at 95% with the Spearman test. The correlations between both reanalyses over their common years of overlap are shown (r-value).

280x148mm (300 x 300 DPI)

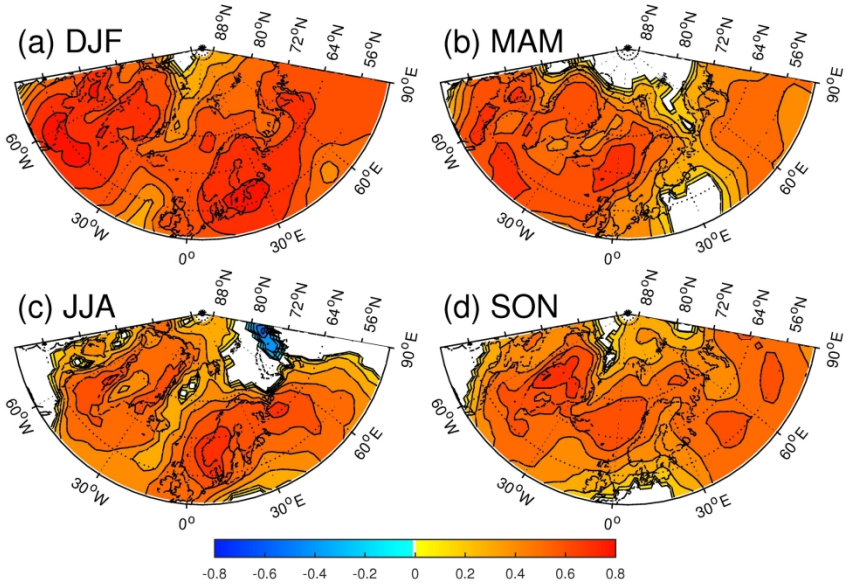

Figure 3. Inter-annual correlation coefficients between OBS and EXP 2m temperature dataset from 1951 to 2014 for a) winter b) spring c) summer and d) fall. Only grid points where correlations are significant at 95% confidence are shown.

225x140mm (300 x 300 DPI)

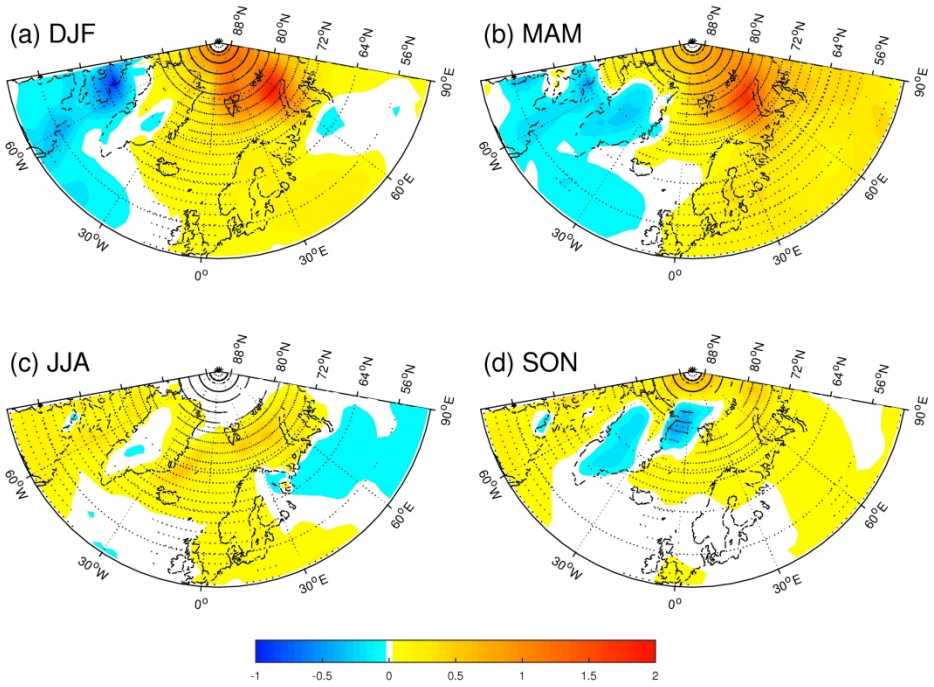

Figure 4. Evolution of 2m temperature (°C per decade) from 1951 to 2014 from the CTL dataset for a) winter b) spring c) summer and d) fall. The dotted areas represent values that show linear regression coefficients of temperatures significant at 95% confidence level with the Spearman test.

274x200mm (300 x 300 DPI)

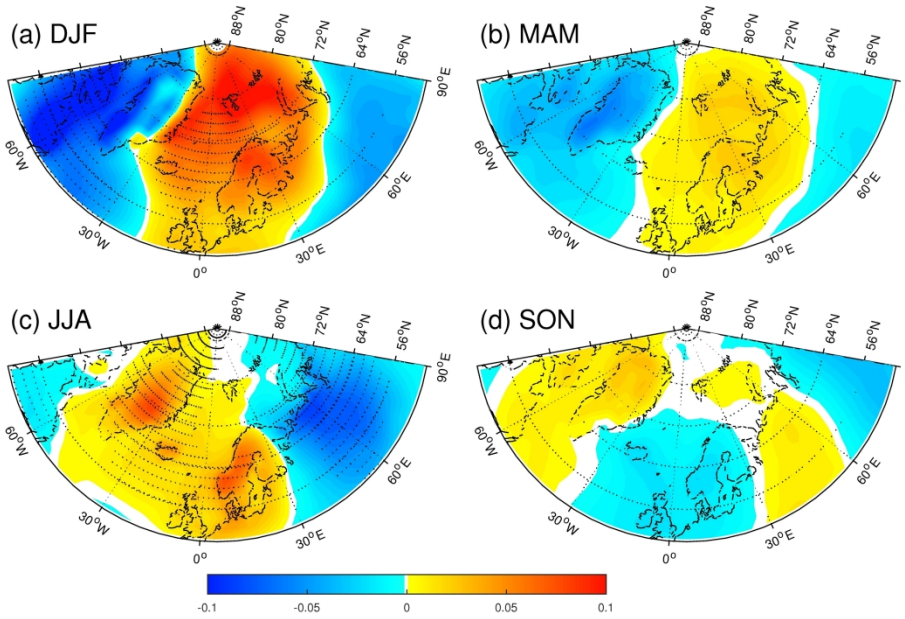

Figure 5. Evolution of 2m temperature from 1951 to 2014 from the EXP dataset for a) winter b) spring c) summer and d) fall. The dotted areas represent values that show linear regression coefficients of temperatures significant at 95% confidence level with the Spearman test.

272x182mm (300 x 300 DPI)

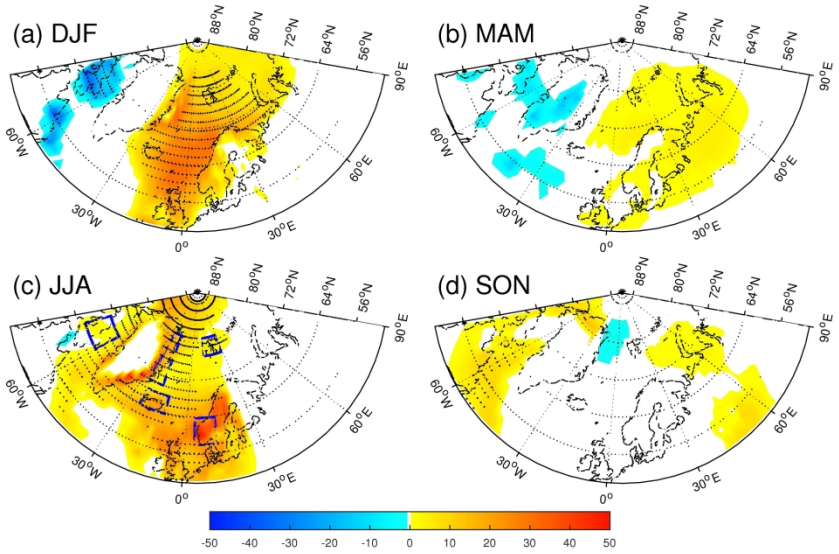

Figure 6. Percentage of warming (reds) or cooling (blues) represented by the EXP dataset compared to CTL averaged for all 10 combinations (see text) for a) winter b) spring c) summer and d) fall. The grid points shown are those with the same sign in EXP and CTL (warming or cooling) and significant change of CTL at 95% confidence level with Spearman. The dotted points represent grid points where the standard deviation is lower than 25% of the 10 combinations average.

279x165mm (300 x 300 DPI)

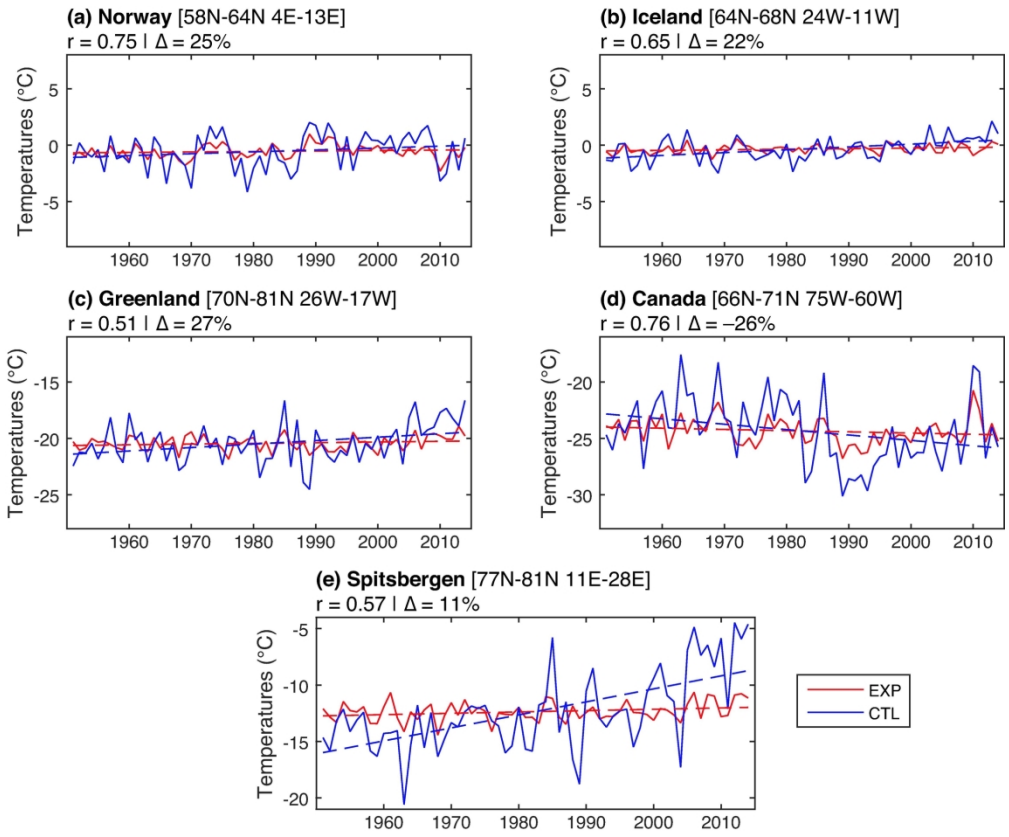

Figure 7. Inter-annual evolution of CTL and EXP temperatures dataset in winter for a) Norway b) Iceland c) eastern Greenland d) northeastern Canada and e) Spitsbergen shown as blue boxed areas on Figure 6c. Interannual correlations between EXP and CTL (r-value) and the ratio between the increase of EXP and the increase of CTL averaged for all grid points (Δ) are also shown.

193x160mm (300 x 300 DPI)

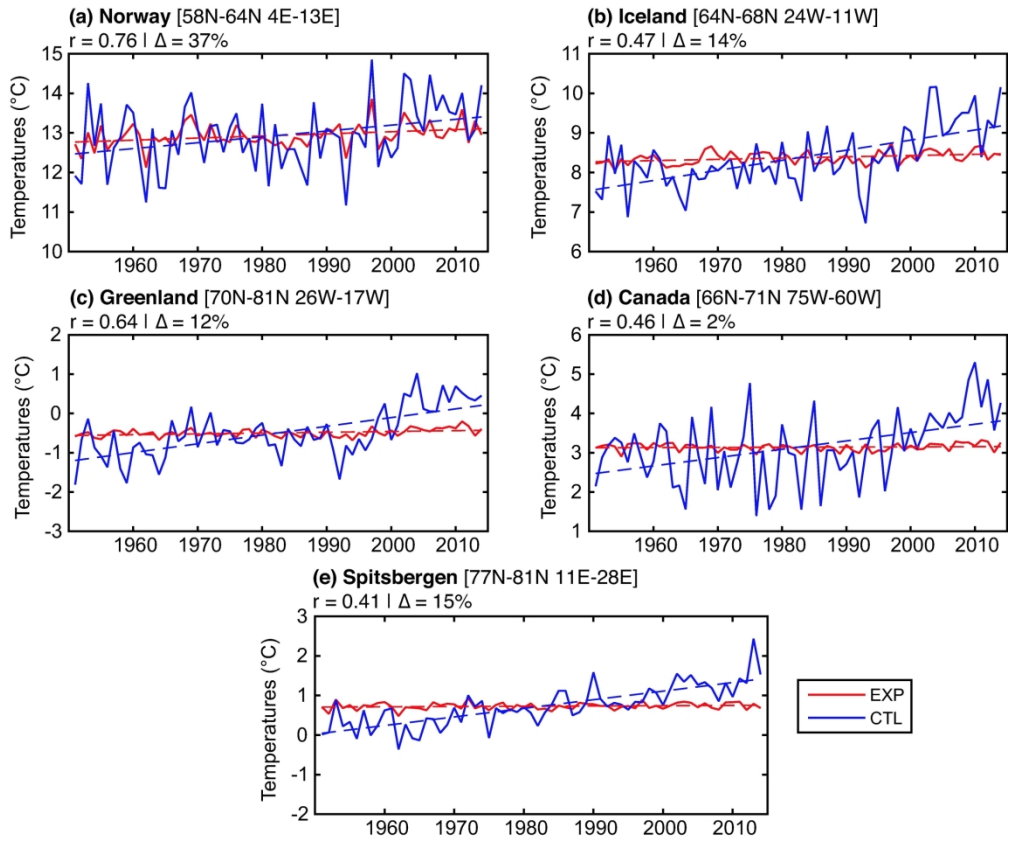

Figure 8. Inter-annual evolution of CTL and EXP temperatures dataset in summer for a) Norway b) Island c) eastern Greenland d) northeastern Canada and e) Spitsbergen shown as blue boxed areas on Figure 7c. Interannual correlations between EXP and CTL (r-value) and the ratio between the increase of EXP and the increase of CTL (Δ) are also shown.

198x165mm (300 x 300 DPI)

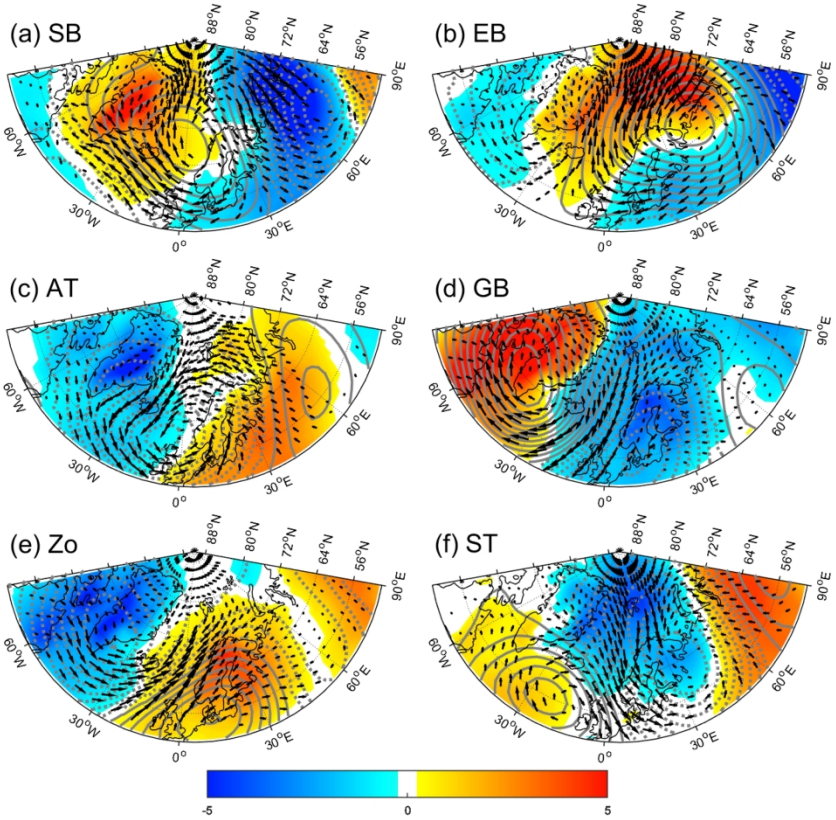

Figure 9. Winter 20CR 2m temperature anomalies in °C (colors),Z500 anomalies (Greylines, in intervals of 20m, dashed lines indicate negative values) and 10m wind anomalies (black vectors) corresponding to each regime from 1951 to 2014. All anomalies are significant at the 95% confidence level according to t-test

278x250mm (300 x 300 DPI)

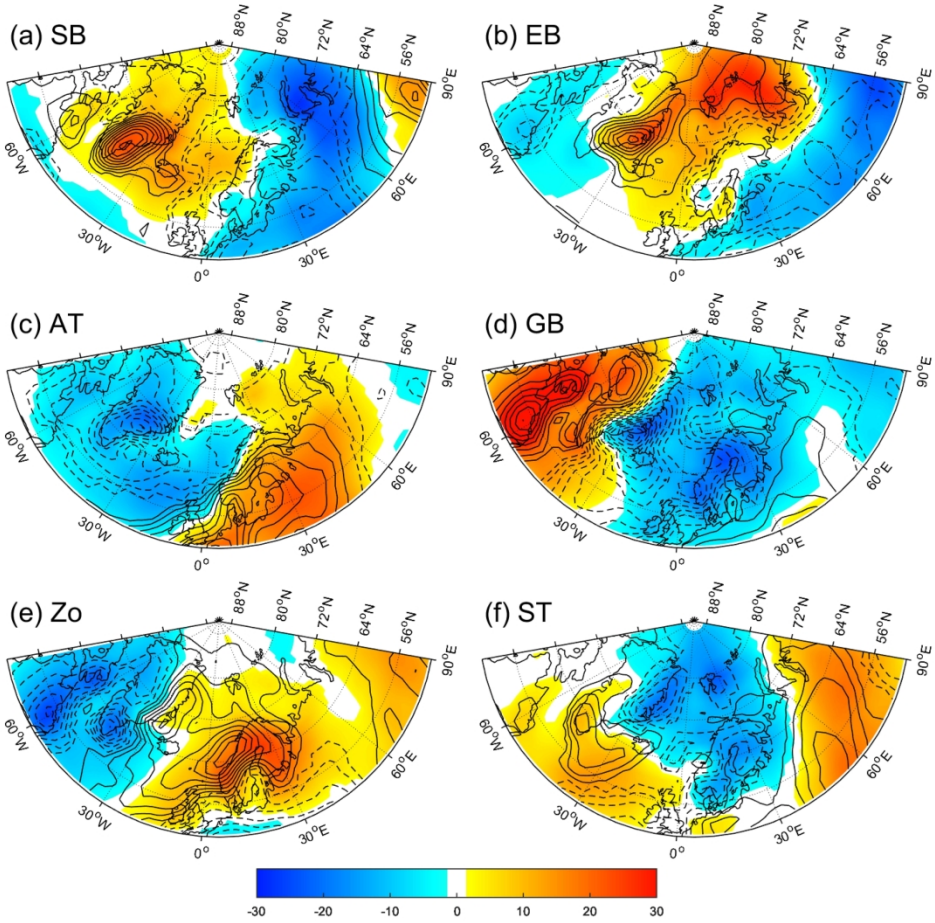

Figure 10. Winter 20CR downward IR anomalies in W/m2 (shading) and cloud water content anomalies (Black lines, in 5g/m2 intervals, dashed lines indicate negative values) corresponding to each regime from 1951 to 2014. All anomalies are significant at the 95% confidence level according to t-test

261x250mm (300 x 300 DPI)

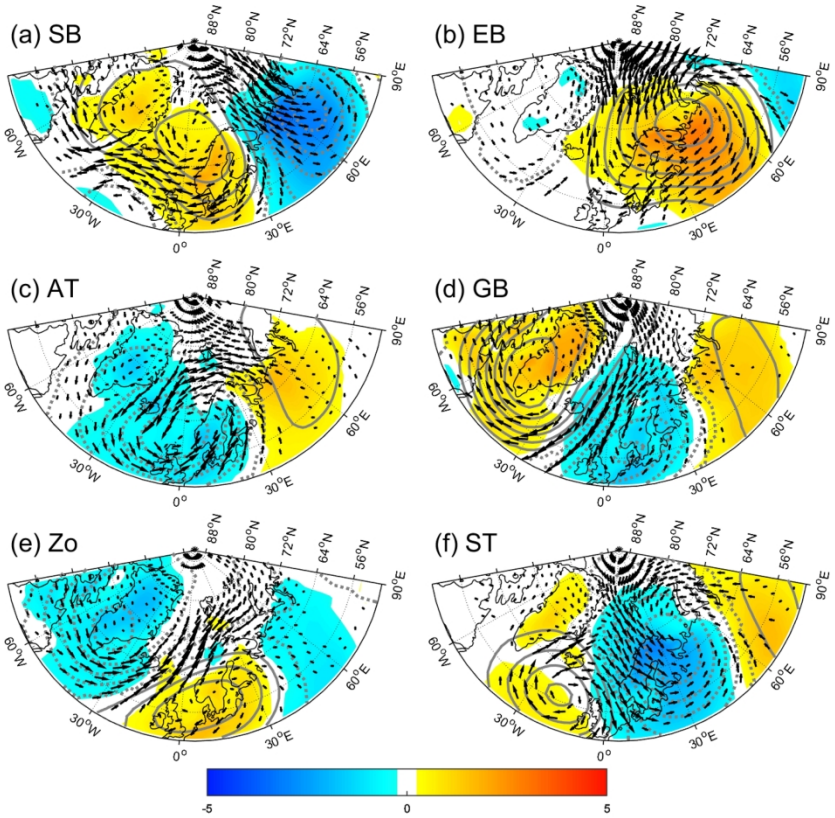

Figure 11. Summer 20CR 2m temperature anomalies in °C (shading),Z500 anomalies (Gray lines, in intervals of 20m, dashed lines indicate negative values) and 10m wind anomalies (black vectors) corresponding to each regime from 1951 to 2014. All anomalies are significant at the 95% confidence level according to t-test

279x250mm (300 x 300 DPI)

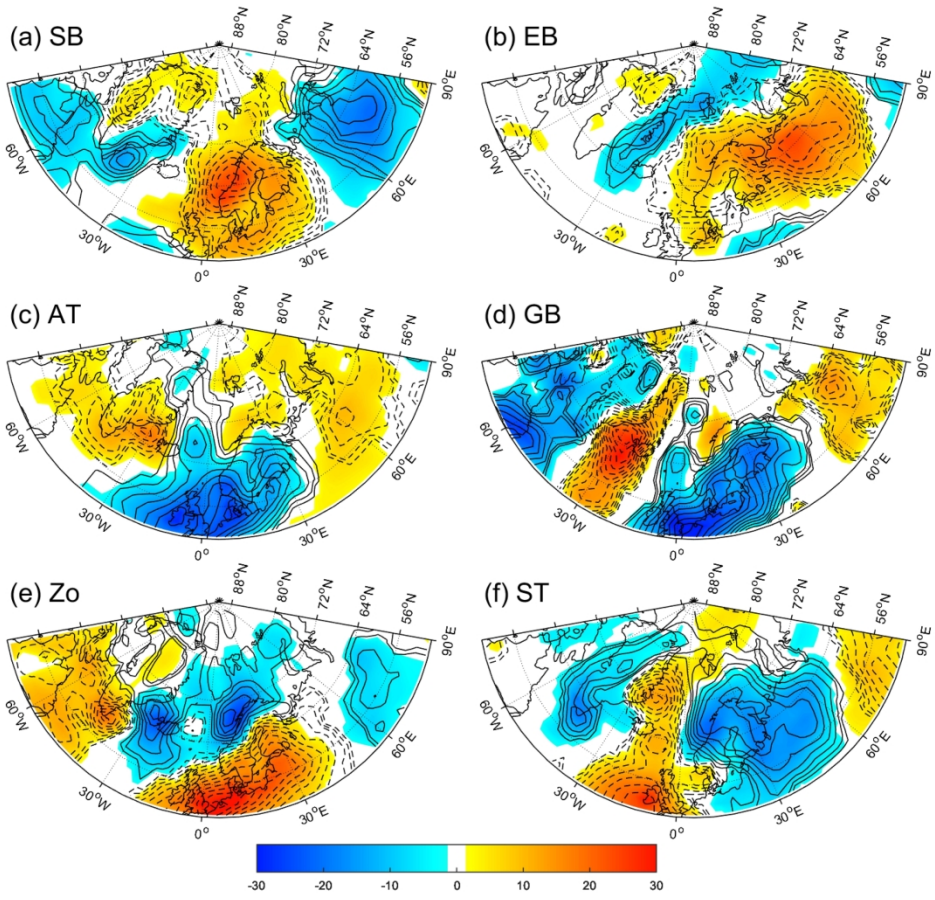

Figure 12. Summer 20CR downward SR anomalies in W/m2 (shading) and cloud cover percent anomalies (black lines, in interval of 1%, dashed lines indicate negative values) corresponding to each regime from 1951 to 2014. All anomalies are significant at the 95% confidence level according to t-test

270x250mm (300 x 300 DPI)

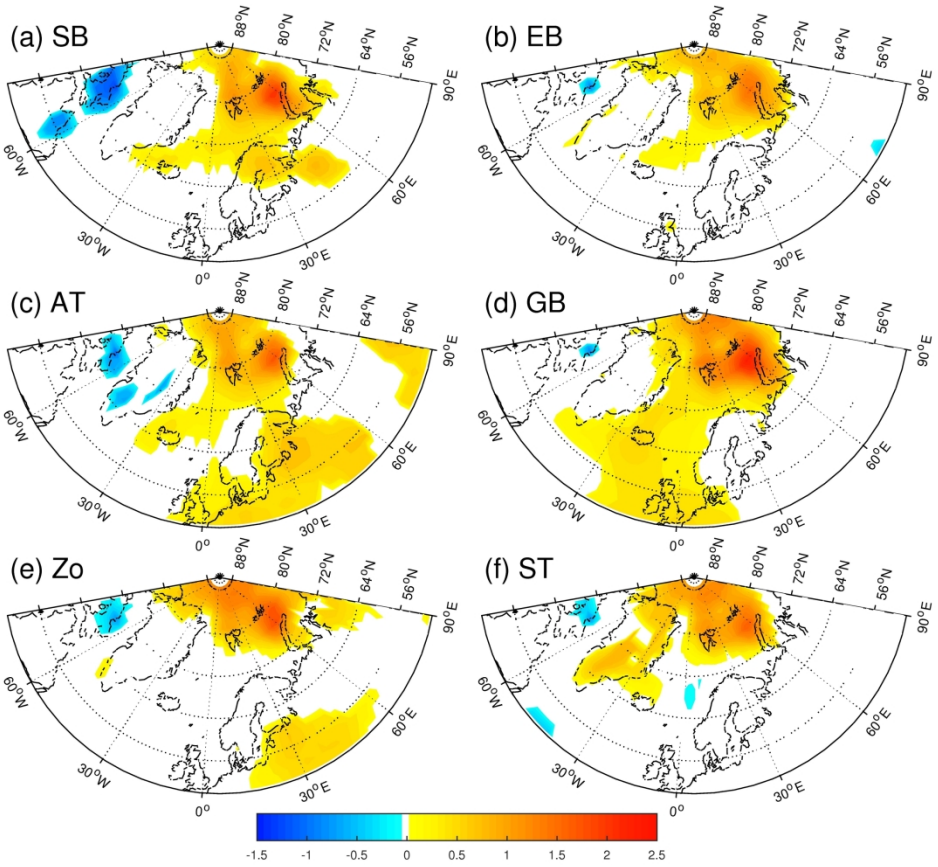

Figure 13. Evolution of 20CR 2m temperature (°C per decade) from 1951 to 2014 for each regime in winter. Only grid points with an evolution of temperatures significant at 95% confidence level with the Spearman test are shown.

256x227mm (300 x 300 DPI)